EPR AND OPTICAL STUDY OF SiO_2 FILMS IMPLANTED WITH GERMANIUM IONS

V.YA. BRATUS', M.YA. VALAKH, E.G. GULE, S.M. OKULOV, V.O. YUKHYMCHUK

Institute of Semiconductor Physics, Nat. Acad. Sci. of Ukraine
(45, Nauky Prosp., Kyiv 03028, Ukraine; e-mail: v_bratus@isp.kiev.ua)

UDC 538.955; 535.337

Electron paramagnetic resonance (EPR) and photoluminescence (PL) have been used to study SiO_2 films grown by thermal oxidation of silicon substrates and possessing either a homogeneous distribution or that close to a Gaussian one of implanted Ge atoms. The E'_γ centers connected with oxygen vacancies in SiO_2 and the defects induced by replacing Si atoms in the matrix sites by Ge ones have been identified as dominant paramagnetic defects. Among the latter, the Ge E' and Ge(2) centers, as well as the germanium peroxy radical Ge PR, have been recognized. The fact that the concentration of defects in specimens with a homogeneous distribution of Ge atoms was an order of magnitude lower than that in specimens with a Gaussian distribution has been explained by a dynamic annealing of defects during the multiple implantation. The revealed correlation between the intensity variations of EPR spectra and PL bands peaked at 1.94, 2.00, and 2.20 eV, which took place at annealing, testifies to that those bands are of the defect nature. At the same time, the PL band with a maximum at 2.32 eV, which appeared after annealing at 900 °C, has been connected with the formation of Ge nanocrystallites in SiO_2.

1. Introduction

Bulk germanium and silicon are indirect-gap semiconductors with a low efficiency of interband emission in the infra-red (IR) range, which does not allow them to be used for the manufacture of emitters for optoelectronic devices. However, if the dimensions of Si and Ge crystallites are reduced to several nanometers, a variation of a lot of properties including the energy spectrum takes place, owing to the size quantization [1]. For example, the observation of visible PL becomes possible because the emergence of quantum levels in crystallites and substantial modifications of the electronic structure that is typical of bulk materials considerably enhance the efficiency of emission at room temperature. For this reason, significant efforts of researchers have been directed for the last decade at studying the effects of size quantization and developing the integrated optoelectronic silicon-based devices.

According to the elementary theory of size quantization, which is based on the method of effective mass [1], the shift E_R of the conduction band edge in a semiconductor sphere with radius R, which is smaller than the effective Bohr radius of an exciton a_B, towards shorter waves with respect to its position in a bulk semiconductor is equal to $E_R = \pi^2 h^2/2\mu R^2$, where μ is the reduced effective mass of an exciton. The effective Bohr radius of excitons in Ge, $a_B \approx 24$ nm, is larger than that in Si, $a_B \approx 10$ nm, while the effective masses of electrons and holes are smaller [2]. Therefore, more substantial variations of the electronic structure should be expected to occur in Ge quantum dots as compared to those in Si quantum dots similar by dimensions. A lot of technological methods followed by thermal annealing are used to form germanium nanocrystallites (nc-Ge) in a SiO_2 matrix: magnetron sputtering of SiO_2 and Ge plates [3], oxidation of $Si_{1-x}Ge_x$ alloys [4], molecular beam epitaxy [5], chemical vapor deposition [6], implantation of Ge^+ ions [7], and so on. An important advantage of the last quoted method is the exact monitoring over the concentration of implanted atoms and the profile of their distribution in a SiO_2 matrix, and its full compatibility with industrial microelectronic technologies. However, during the ion implantation, there appear radiation-induced defects, because of which the radiative recombination of current carriers may also take place [8].

Irrespective of the method applied for synthesizing nc-Ge in SiO_2, the bands close by position have been observed in the corresponding PL spectra. Depending on the excitation energy, some bands of emission have been detected in a range from near ultraviolet to near IR (see, e.g., [7, 9]). The PL bands with energies of 4.3 and 3.1 eV are attributed to transitions between the energy levels of a neutral oxygen vacancy in SiO_2, surrounded by two Ge atoms [7], i.e. with a defect in the SiO_2 matrix. The origin of other PL bands has not been elucidated ultimately. For their explanation, various authors involved the mechanisms of both the exciton recombination under the conditions of confinement [10] and the recombination of current carriers through defective states at the nc-Ge/SiO_2 interface [11] and in the SiO_2 matrix [12] under consideration.

In general, the availability of defects of various origins, including paramagnetic ones, has been supposed in works devoted to the research of Ge^+-implanted SiO_2 films. Some preliminary results of EPR measurements carried out on those objects have been reported earlier [13,14]. This work aimed at elucidating the basic types of paramagnetic defects and their evolution during thermal annealing of SiO_2 films, where various distribution profiles of germanium atoms had been formed by the ion implantation.

2. Experimental Method

The SiO_2 films 500 or 1000 nm in thickness were grown on silicon (100) plates by thermal oxidation of the latter in the atmosphere of humidified oxygen. Specimens with three different distribution profiles of implanted germanium ions in the SiO_2 film were investigated. In all the cases, the profile was calculated using a TRIM-98 computer program [15]. The specimens of the first type (I) were characterized by a homogeneous distribution of germanium atoms in the 500-nm SiO_2 film. The distribution was created by consecutive implantations of Ge^+ ions, with the corresponding ion energy E and the expose dose D at every stage being $E_1 = 150$ keV and $D_1 = 9.0 \times 10^{15}$ cm^{-2}, $E_2 = 100$ keV and $D_2 = 5.4 \times 10^{15}$ cm^{-2}, $E_3 = 50$ keV and $D_3 = 4.3 \times 10^{15}$ cm^{-2}, and $E_4 = 20$ keV and $D_4 = 2.1 \times 10^{15}$ cm^{-2}. The total dose amounted to $D_{\rm I} = 2.08 \times 10^{16}$ cm^{-2}. Under such conditions, the average concentration of Ge atoms at depths of $12 - 120$ nm reckoned from the SiO_2 surface, according to the calculations carried out using the TRIM program, was $N_{\rm Ge} \approx 3$ at.%. In other specimens of this type, the value $N_{\rm Ge} \approx 5$ at.% was achieved by a proportional increase of the expose dose at each stage, with the total dose being 3.48×10^{16} cm^{-2}. The specimens of the second type (II) had a homogeneous distribution of Ge atoms located deeper in an oxide film 1000 nm in thickness. They underwent a three-stage implantation procedure with Ge^+ ions with the energies and doses $E_1 = 400$ keV and $D_1 = 3.0 \times 10^{16}$ cm^{-2}, $E_2 = 300$ keV and $D_2 = 1.0 \times 10^{16}$ cm^{-2}, and $E_3 = 200$ keV and $D_3 = 3.5 \times 10^{16}$ cm^{-2} at each stage, respectively. The total expose dose was $D_{\rm II} = 7.5 \times 10^{16}$ cm^{-2}. In these specimens, the average concentration of Ge atoms at a depth of 360 nm from the SiO_2 surface was about 3 at.%. At last, in the specimens of the third type (III), Ge^+ ions with an energy of 430 keV were implanted into the 1000-nm SiO_2 film up to a dose $D_{\rm III} = 4.1 \times 10^{16}$ cm^{-2}. In this case, the calculations gave the distribution profile of the implanted Ge impurity

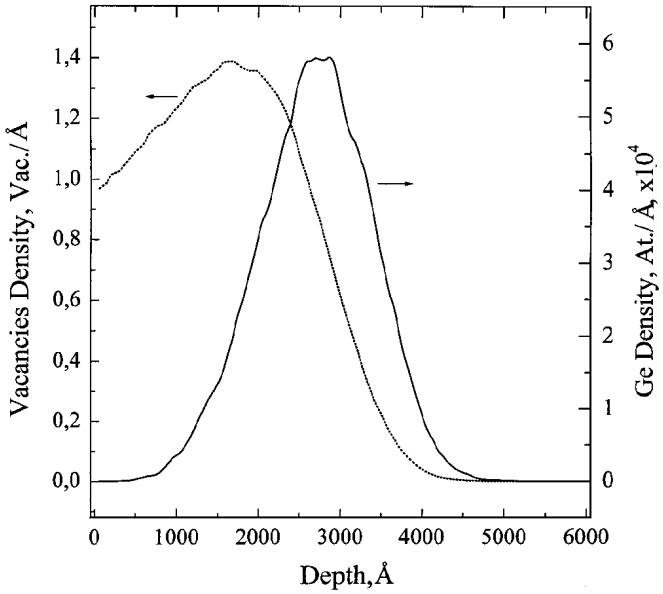

Fig. 1. Distribution profiles of Ge atoms and vacancies in a SiO_2 film implanted with Ge^+ ions with an energy of 430 keV, calculated using a TRIM-98 program. The SiO_2 film density $d = 2.26$ g/cm^{-3} and the effective threshold energies for displacement of silicon and oxygen atoms $E_d = 22$ eV were used in calculations

that was close to a Gaussian one (Fig. 1) with the values of the mean projected range and straggle spread of 269 and 67 nm, respectively. The peak concentration of Ge atoms was about 4 at.%.

The annealing procedure of implanted specimens in a nitrogen environment was carried out consistently within the temperature interval from 100 to 1100 °C and with a step of 100°C. The time of annealing was 15 min.

The EPR spectra were measured using medium-size $0.5 \times 3 \times 15$-mm^3 specimens. The measurements were carried out at room temperature, in the X-range (the microwave frequency $\nu \sim 9.4$ GHz), and with a 100-kHz modulation of the magnetic field. In order to prevent the effects of saturation and overmodulation, the averaging over 16 to 49 spectra was fulfilled while registering the relatively narrow EPR lines with small intensities. In general, the microwave power did not exceed 1 mW and the amplitude of modulation of the magnetic field was at most 0.06 mT during experimental measurements. In order to compare the parameters of various specimens and to estimate quantitatively the g-factor and the concentration of defects, a researched specimen and a reference one, MgO:Mn^{2+} with the known number of spins, were placed together into a microwave resonator. The number of defects was determined by comparing

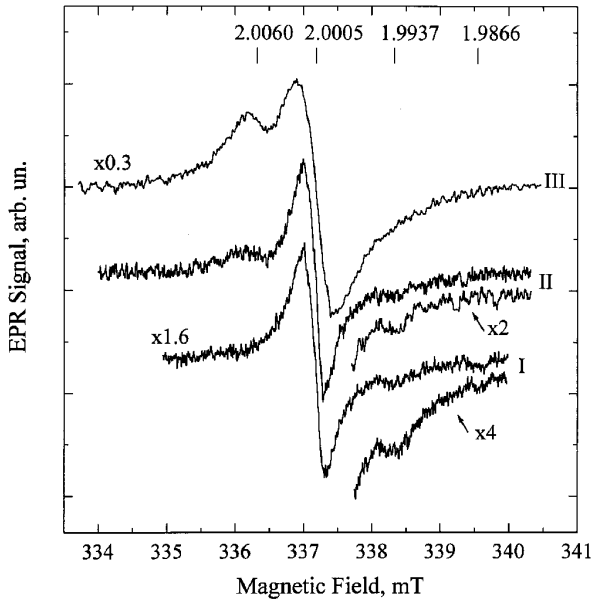

Fig. 2. EPR spectra of defects in SiO_2 films with different distribution profiles of germanium atoms (specimens of types I—III). All spectra were measured under the same conditions at room temperature and normalized per unit surface area of the specimen, $\nu = 9.441$ GHz. The positions of spectrum peculiarities are marked by vertical strokes with corresponding values of the g-factor

the double integrals of the first derivatives of the absorption signals registered on the investigated and reference specimens. The absolute error of the defect number evaluated in such a way amounted to ±40%. At the same time, when comparing various specimens, the relative error did not exceed ±15%.

The PL spectra in the range from 500 to 800 nm were registered at room temperature on a DFS-24 double monochromator, with the emission of an Ar^+ laser ($\lambda =$ 487.9 nm), being used for their excitation. In the range from 360 to 600 nm, we used a nitrogen laser with $\lambda = 337.18$ nm to excite PL spectra and a KSVU-31 installation to study them.

3. Results and Their Discussion

No EPR signal was detected from those parts of the SiO_2/Si structures that did not undergo implantation. In Fig. 2, the EPR spectra measured for all three types of as-implanted specimens and normalized per unit surface area of the specimen are presented. They are composed of several lines, with an almost symmetric line with $g = 2.0005 \pm 0.0002$ being dominating in all of them. In the specimens of types I and II with a homogeneous distribution of implanted Ge atoms, this line had identical forms and almost identical amplitudes. At the same time, it was considerably wider and more intensive in the specimens of type III. In the course of annealing (Fig. 3), this line acquired the form that could be simulated by the parameters of the E'_γ defect (Fig. 4), which was connected with oxygen vacancies in amorphous SiO_2 ($g_1 = 2.0018$, $g_2 = 2.0006$, and $g_3 = 2.0003$ [16]). The structure of the latter is adopted to be represented as $O_3{\equiv}Si\bullet\ {}^+Si{\equiv}O_3$, where the symbols "•", "+", and "≡" stand for an unpaired electron, a hole, and bonds with three separate oxygen atoms, respectively. According to calculations [17], such a structure can arise provided that a hole is trapped by a neutral oxygen vacancy or an O^- ion is shifted from the site. As a result, the electron would be localized on the broken sp^3-orbital of the Si atom, whereas the positively charged atom of silicon located on the opposite side of the vacancy would possess sp^2 hybrid orbitals and relax into a plane of three oxygen atoms [17].

The lines with lower intensities were distinctly observed on the tails of the EPR spectrum of the E'_γ defect (Fig. 2). The line in the vicinity of the value $g = 1.99370 \pm 0.0003$ was distinctly registered in unannealed specimens of types I and II. During annealing, its intensity decreased more slowly than that of the spectrum of the E'_γ defect did (Fig. 3,*a*; see also work [14]), which allowed us to observe this line also in specimens of type III after their annealing at 400°C (Fig. 3,*c*). The value of 1.9937 for the g-factor means that this line can correspond to the value g_3 of the so-called Ge E' defect ($g_1 = 2.0012$, $g_2 = 1.9954$, and $g_3 = 1.9937$ [18]). This defect was observed in both irradiated germanium glass [18] and an optical Ge-doped quartz fiber [19] and is an analog of the E' center in SiO_2. Accordingly, its structure can be represented as $O_3{\equiv}Ge\bullet\ {}^+Ge{\equiv}O_3$.

The line with $g = 1.9866 \pm 0.0003$ was observed only in unannealed specimens of type I (Fig. 2). It may correspond to the value g_3 of the Ge(2) defect ($g_1 =$ 2.0010, $g_2 = 1.9978$, and $g_3 = 1.9868$ [20]), the origin of which has not been elucidated ultimately. It is supposed [19] that a replacement of silicon by germanium in the SiO_2 structure introduces traps for electrons, so that the so-called fourfold coordinated germanium electronic center Ge(2) has a structure $O_3{\equiv}Ge^\bullet{-}O{-}Ge{\equiv}O_3$ with Si atoms in the following spheres. In a later work [21], the Ge(2) center was classified as a hole trapped by a defect, which appeared due to the formation of two oxygen vacancies in the vicinity of a Ge impurity in SiO_2 followed by pairing of two orbitals. The structure of this center, the so-called twofold coordinated Ge atom in

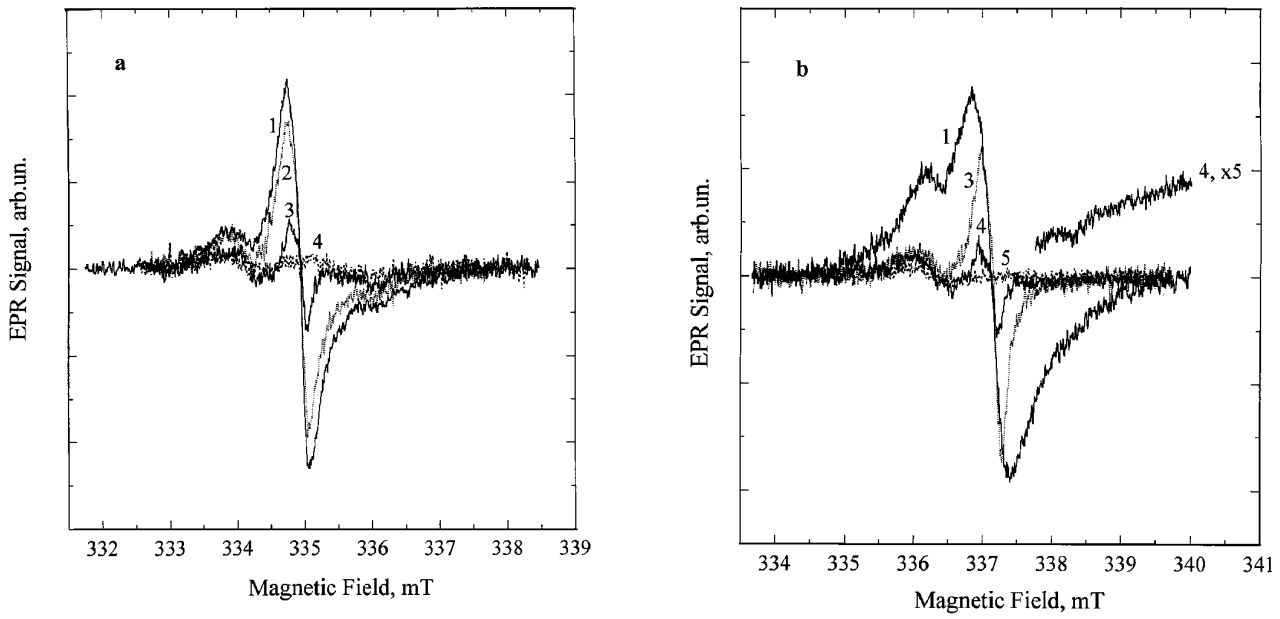

Fig. 3. EPR spectra of specimens of type II (panel *a*, ν = 9.378 GHz) and III (*b*, ν = 9.441 GHz): as-implanted specimens (*1*) and specimens consistently annealed in the nitrogen environment for 15 min at temperatures of 200 (*2*), 300 (*3*), 400 (*4*), and 500°C (*5*)

SiO_2, can be represented as $(—O—Ge^{\bullet\bullet}—O—)^+$, where the symbol "$\bullet\bullet$" denotes coupled orbitals.

The line corresponding to $g = 2.0060 \pm 0.0002$ was observed in specimens of types II and III (Fig. 2), where ions were implanted into a 1000-nm SiO_2 film. A characteristic feature of this line was that its intensity did not reach saturation as the microwave power grew up to 100 mW and became almost twice as large after the specimen had been annealed at 300 °C (Fig. 3). Such a behavior and a position of the line are inherent to a peroxy radical GePR in irradiated germanium glass and GeO_2 powder ($g_1 = 2.0020$, $g_2 = 2.0062$, and $g_3 = 2.0312$ [18,22]), the structure of which can be represented as $O_3{\equiv}Ge—O—O\bullet$. In specimens of type I prepared on the basis of 500-nm SiO_2 films, on the contrary, a very weak EPR line from a nonbridging oxygen hole center (NBOHC) [14] ($g_1 = 2.0020$, $g_2 = 2.0080$, and $g_3 = 2.0510$ [22]), the structure of which is represented as $\equiv Ge—O\bullet\ ^+Si\equiv$, was observed. It was found for quartz glass [23] that a similar PR defect appears in specimens with a small content of OH groups as a result of the breaking of the peroxy chain $\equiv Si–O–O–Si\equiv$, whereas the NBOHC emerges in specimens with a high content of OH groups as a result of the breaking of strained bonds $\equiv Si—O—Si\equiv$. Thus, some distinctions between EPR spectra for specimens of different types may be connected to different contents of OH groups in oxide films possessing different thicknesses.

It should be noted that the presence of the intensive E'_γ line in the g-factor interval 2.0020 – 1.9999 of the spectra of unannealed specimens, where one should expect the appearance of the characteristic lines of defects connected with Ge, and some broadening of lines in the vicinity of the g_3 values for the Ge PR and NBOH centers [18,22], hampers the observation of separate lines in EPR spectra. A considerable reduction of the intensity and a narrowing of the E'_γ line after the annealing of the specimens simplify the simulation of the spectra observed, as is illustrated in Fig. 4. In order to calculate the E'_γ, GeE', and GePR components of the spectrum, we used the values of the g-factors quoted above, while the distributions of the g_2 and g_3 values were taken from works [24] and [18], respectively. The ratios between the integrated intensities of the E'_γ, GeE', and GePR amounted to approximately 1:2:4 for the example concerned. All the mentioned defects had been found earlier in Ge-doped quartz glass, an optical fiber, or, except for E'_γ, germanium glass. Their observation in the EPR spectra of unannealed implanted SiO_2 films indicates that Ge atoms were built abundantly into the matrix instead of Si atoms without thermal activation. Earlier, it was evidenced by IR absorption and X-ray photoelectron spectroscopy measurements [25].

Important conclusions can be drawn by analyzing the quantitative results concerning the concentration of

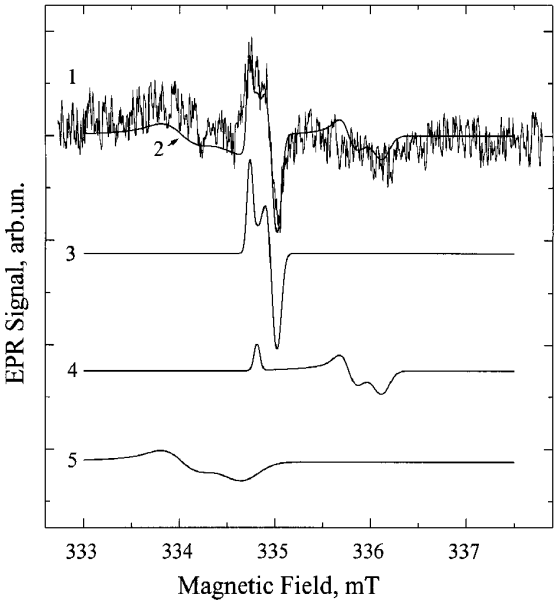

Fig. 4. The EPR spectrum of a specimen of type II annealed at 300 °C (*1*). The frequency $\nu = 9.378$ GHz, the temperature of observation $T = 300$ K. The calculated spectrum (*2*) is a superposition of the components from three defects: the E'_γ (*3*), Ge E' (*4*), and Ge PR ones (*5*). The spectroscopic parameters of simulation are quoted in the text

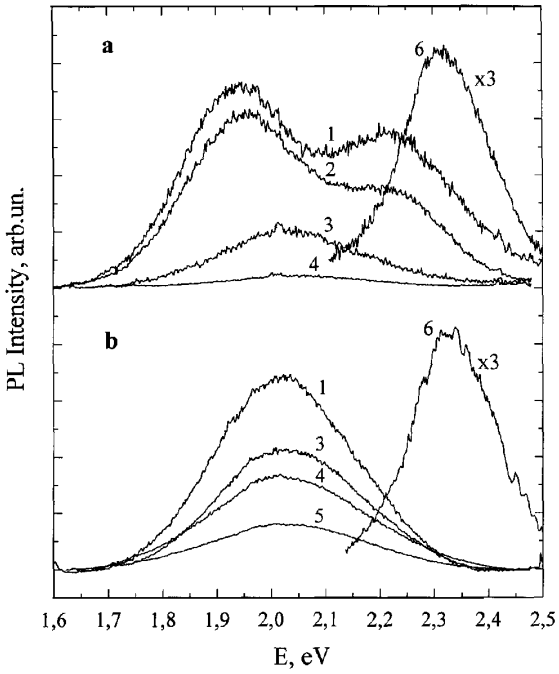

Fig. 5. PL spectra ($E_{ex} = 2.54$ eV) of $Ge^+/SiO_2/Si$ structures of types II (*a*) and III (*b*): an as-implanted specimen (*1*) and specimens consistently annealed in the nitrogen atmosphere for 15 min at temperatures of 200 (*2*), 300 (*3*), 400 (*4*), 500 (*5*), and 900 °C (*6*)

defects in unannealed and annealed specimens. Some experimental parameters of implanted specimens and those calculated with the help of a TRIM computer program are quoted in the Table. Considering the table data, two points attract attention. It is, first, close values of the total numbers of paramagnetic (PM) defects per unit surface area N_S in specimens of types I and II with $N_{Ge} \approx 3$ at.%, in spite of the fact that the homogeneous distribution of Ge in specimens of type II was created by applying the considerably larger energies and doses of implanted ions. We note that, for specimens of type I with different doses of implantation, a definite proportionality was revealed, namely, the value of N_S for a specimen with $N_{Ge} \approx 5$ at.% is half as much again as for a specimen with $N_{Ge} \approx 3$ at.%. Secondly, it is the value of N_S for the specimens of type III, which was almost one order of magnitude larger than that for the specimens of type II, provided that the total dose of implanted ions into the former was almost half as much and the doses of high-energy ions were close. It is also worth noting that, besides vacancies that were created when high-energy ions collided elastically with nuclei, additional defects arose in SiO_2 in the course of energy loss of those ions by electron excitation (for example, it was equal to about 30% in the case of Ge^+ implantation with $E = 430$ keV). The defect formation efficiency in inelastic processes was two orders of magnitude as low, but they can also result in the breaking of Si–O bonds [26].

A high-dose implantation may lead to the formation of a considerable number of defects and their associates

Some experimental and theoretical (designated by *) parameters of unannealed specimens $Ge^+/SiO_2/Si$. Theoretical parameters were calculated making use of a TRIM program

Specimen type	Energy of ions Ge^+ E, keV	Total dose D_Σ, cm^{-2}	Vacancy distribution* ΔX_d, nm	Number of PM defects N_S, cm^{-2}	Concentration of PM defects* N_V, cm^{-3}
I	150 + 100 + 50 + 20	2.1×10^{16}	101	1.6×10^{15}	1.6×10^{20}
II	400 + 300 + 200	7.5×10^{16}	287	2.0×10^{15}	7.0×10^{19}
III	430	4.1×10^{16}	269	1.5×10^{16}	5.6×10^{20}

in both the paramagnetic and diamagnetic states [27]. In addition, a reduction of the number of vacancies may occur by their annihilation while interacting with interstitial atoms. The so-called dynamic annealing of defects, which was not taken into account in a TRIM program, may occur during the implantation owing to an elevated temperature. For specimens of all types, the ion current density that was used in the course of implantation did not exceed 0.03 μA/cm^{-2}. The corresponding supplied thermal power was rather insignificant to heat up a specimen. According to the estimations carried out with the use of the formulae of work [27], even when implanting ions with an energy of 430 keV, the temperature of a specimen cannot raise by more than 15 °C. At the same time, a local rise of the temperature stimulated by accidental cascades of collisions was quite probable provided that the heat conductivity of SiO_2 is low. Concerning the possible annihilation of defects, when a specimen was being stored at room temperature, we know only the literature data regarding the low-temperature annealing of E' and NBOHC defects due to the diffusion of molecular hydrogen after irradiation of fused quartz at 130 K [23].

The EPR studies testified to that a substantial reduction of the number of paramagnetic defects occurred as a result of the multiple implantations carried out to create a uniform distribution profile of dopants. It is known [27] that the maxima of distributions of radiation-induced damages X_d and implanted atoms R_p do not coincide. For example, it followed from TRIM calculations (Fig. 1) that, in the case of the implantation of Ge^+ ions with the energy $E = 430$ keV into SiO_2, the relation $X_d \approx 0.6R_p$ was actual. As is seen from Fig. 1, a recession of the damage distribution curve towards the surface is characterized by a very sluggish gradient, so that the concentration of vacancies near the surface amounts to 70% of the peak value. It allowed us to divide the damaged area of the SiO_2 film conventionally into two layers, nonsaturated and saturated with implanted atoms, both being approximately equal by volume. Judging from a reduction of the number of defects in specimens of type II as compared with that in specimens of type III, it is possible to suggest that in the course of the further cascades of collisions of implanted ions possessing a lower energy in the previously nonsaturated layer, the formation of new defects was accompanied by their more effective dynamic annealing. The latter was promoted by a relative increase of the energy that was supplied to the phonon subsystem, i.e. was spent for heating the matrix, as the energy of ions diminished. At last, a reduction of the number of defects might also be favored by a replacement of vacant sites of the lattice by implanted atoms, which our observations of paramagnetic defects connected with Ge in unannealed specimens evidenced for. In general, when creating a uniform profile of the impurity distribution by multiple ion implantations, the sequence with the descending order of ion energies is preferred. For a crystal matrix, it occurs first of all because of the following fact. If a series of implantations was carried out with the descending order of ion energies, a consecutive damage of the surface layer would take place, which might result in the scattering of high-energy ions into channeling directions (see, e.g., [28]). Surface sputtering is another factor that can result in a loss of impurities implanted preliminary at low energies. As follows from our results, multiple implantations with the consecutive decreasing of the ion energy also led to a substantial decrease of the defect concentration.

The values of the bulk concentration of defects N_V, which are presented in the Table, are evaluative and were calculated using their experimentally determined number N_S and the average width ΔX_d of the vacancy localization region by the relation $N_V = N_S/\Delta X_d$. The value of ΔX_d was selected, according to TRIM calculations, as a width of the vacancy distribution at its half maximum. The results of such an estimation of the bulk concentration N_V make clear a significant broadening of the E'_γ spectra in unannealed specimens, especially those of type III. Similarly to the case of SiO_2 films implanted with Si^+ ions [8], a contribution of the dipole-dipole interaction between nearly located pairs to the width of the EPR line and an influence of the stresses that arise when implanted layers become oversaturated with vacancies and interstitial atoms on the distribution of g-factors [29], were considerable at such high concentrations of defects. The annealing of specimens led to a gradual reduction of the concentration of defects, which had an expressive effect, first of all, on the width of the most intensive line E'_γ (Fig. 3).

Distinctions between specimens of different types and a certain correlation with EPR data were also observed for PL spectra. Similarly to works [7, 30], a band with the maximum of about 2.93 eV was registered in the PL spectra of unannealed specimens of all three types; the specimens were excited by the emission of a nitrogen laser ($E = 3.68$ eV). In accordance with the results of work [7], as the annealing temperature of the specimens grew up to 500°C, the intensity of this band increased considerably. The further annealing resulted in a gradual reduction of the PL intensity, and the band was not observed any more after the annealing

at a temperature of 1000 °C. Concerning the nature of this band, the authors of work [7] assign it to a neutral oxygen vacancy surrounded by Ge and Si atoms in various combinations, while the authors of work [30] do with a neutral twofold coordinated germanium center —O—Ge$^{\bullet\bullet}$—O—. The validity of the last assumption has been proved in the later work [21].

It is worth noting that, in the case of PL excitation by the emission of a nitrogen laser, only the band with the maximum near to 3.0 eV was observed in the spectrum, while the bands in the range of 1.9 – 2.2 eV did not appear. If the as-implanted specimens were excited by the emission of an argon laser with the energy of 2.54 eV, two intensive bands with maxima at 2.20 and 1.94 eV were registered in the PL spectra of the specimens of types I and II (Fig. 5,*a*), and an intensive band with the maximum at 2.00 eV was observed for the specimens of type III (Fig. 5,*c*). As one can see from Fig. 5, the annealing of implanted films resulted in a gradual diminishing of the intensity of the indicated PL bands, and, after the annealing at $T_a \geq 600$°C, they were not registered any more analogously to the EPR spectra.

A correlation between intensity changes of the PL and EPR spectra during the annealing of specimens evidences for the defective nature of those bands. Another argument, which supports such a conclusion, is the fact that an analogous correlation takes place between the PL band and the most intensive component E'_γ of the EPR spectra of the SiO_2 films of type III and the SiO_2 films implanted with Si^+ ions with the energy $E = 150$ keV and the dose $D = 9.0 \times 10^{16}$ cm^{-2}, provided that the annealing temperature was less than 700°C. According to TRIM calculations, the profiles of vacancy distribution and vacancy concentration, as well as the widths of the layers nonsaturated with Ge or Si atoms, had to be close. It allowed us to relate the PL band at 2.0 eV to the recombination of radiation-induced defects exactly in the subsurface nonsaturated SiO_2 layer.

The higher concentration of Ge atoms and defects connected to them in specimens of types I and II probably stimulated the PL spectrum with two maxima (Fig. 5). Using the results of X-ray photoelectron spectroscopy measurements carried out for Ge^+-implanted SiO_2 films, the presence of Ge—O bonds was revealed in the GeO and GeO_2 phases [31]. The further annealing resulted in a substantial growth of the number of Ge—Ge bonds and a simultaneous decrease of the number of Ge—O ones. Quantitative and qualitative modifications of the structure of defects, which occurred in the course of the decay of the unstable phase GeO_x and the precipitation of Ge atoms, can be the reason for those variations that were observed in PL spectra. In general, the majority of PL bands in irradiated SiO_2 are related to the recombination through diamagnetic defects; only the band at 1.9 eV is connected with a paramagnetic NBOHC [23]. As was mentioned above, we observed a weak signal from the NBOHC only in an unannealed specimen of type I.

After the further annealing of specimens of all the types at a temperature above 900°C, a band with the maximum at about 2.32 eV appeared in the PL spectra. We associated this band with the formation of Ge nanocrystallites in the SiO_2 matrix. Indeed, as our study of Raman scattering showed [13], after the specimens had been annealed at $T_a = 900$ °C, a characteristic band of Ge—Ge bond vibrations in germanium nanocrystallites, the average dimension of which was equal to 4.5 nm by estimations, appeared in the spectra. Concerning the nature of the PL band, a substantial shift of the maximum of the PL spectrum from 2.1 to 2.4 eV, which accompanied a diminishing of the nc-Ge average size from 8 to 4 nm, allowed the band to be related to the recombination of electron-hole pairs in the quantum dots themselves [3], whereas the results of relaxational measurements [30] yield that there are recombination centers at the nc-Ge/SiO_2 interface.

Thus, SiO_2 films with a uniform distribution of Ge implanted atoms and that close to a Gaussian one have been studied in this work using the EPR method. It has been found that the dominant paramagnetic defects are the E'_γ centers related to the oxygen vacancy in SiO_2 and the defects resulted from occupying the matrix sites by Ge atoms instead of Si ones. Among the defects, the Ge E' and Ge(2) centers as well as a germanium peroxy radical Ge PR have been recognized. The content of defects in specimens with a homogeneous distribution of Ge atoms, which is lower by one order of magnitude as compared with that in specimens with a Gaussian distribution, can be explained by assuming the dynamic annealing of defects in the course of multiple implantations. The correlations observed in the course of annealing between the intensity variations of the EPR spectra and the PL bands with maxima at 1.94, 2.00 and 2.20 eV testify to that those bands have the defective origin. At the same time, the PL band with the maximum at 2.32 eV, which appears after the annealing of specimens at 900 °C, has been related to the formation of Ge nanocrystallites in SiO_2.

The authors consider as a pleasant duty to express gratitude to Prof. Peter Hemment for his supplying them with specimens.

1. *Efros Al.L., Efros A.L.* // Fiz. Tekhn. Polupr. — 1982. — **16**, N 7. — P. 1209 — 1214.
2. *Maeda Y., Tsukamoto N., Yazawa Y. et al.* // Appl. Phys. Lett. — 1991. — **59**, N 24. — P. 3168 — 3170.
3. *Maeda Y.* // Phys. Rev. B. — 1995. — **51**, N 3. — P. 1658 — 1670.
4. *Paine D.C., Caragianis C., Shigesato Y.* // Appl. Phys. Lett. — 1992. — **60**, N 23. — P. 2886 — 2888.
5. *Kanjilal A., Hansen J.L., Gaiduk P. et al.* // Ibid. — 2003. — **82**, N 8. — P. 1212 — 1214.
6. *Baron T., Pelissier B., Perniola L. et al.* // Ibid. — **83**, N 7. — P. 1444 — 1446.
7. *Rebole L., von Borany J., Yankov R.A. et al.* // Ibid. — 1997. — **71**, N 19. — P. 2809 — 2811.
8. *Valakh M.Ya., Yukhimchuk V.A., Bratus' V.Ya. et al.* // J. Appl. Phys. — 1999. — **85**, N 1. — P. 163 — 168.
9. *Zhang J.Y., Wu X.L., Bao X.M.* // Appl. Phys. Lett. — 1997. — **71**, N 17. — P. 2505 — 2507.
10. *Takeoka S., Fujii M., Hayashi S. et al.* // Phys. Rev. B. — 1998. — **58**, N 12. — P. 7921 — 7925.
11. *Wu X.L., Gao T., Siu G.G. et al.* // Appl. Phys. Lett. — 1999. — **74**, N 17. — P. 2420 — 2422.
12. *Min K.S., Shcheglov K.V., Yang C.M. et al.* // Ibid. — 1996. — **68**, N 18. — P. 2511 — 2513.
13. *Yukhimchuk V.A., Valakh M.Ya., Bratus' V.Ya. et al.* // Proc. 24-th Intern. Conf. on the Physics of Semiconductors, Jerusalem (Israel). — 1998. — Section VII(B). — N 48. — P. 1 — 4.
14. *Bratus' V.Ya.* // J. Phys. Studies. — 2003. — **7**, N 4. — P. 413 — 418.
15. *Ziegler J.F., Biersack J.P., Littmark U.* The Stopping and Range of Ions in Solids. — New York: Pergamon Press, 1985.
16. *Warren W.L., Poindexter E.H., Offenberg M. et al.* // J. Electrochem. Soc. — 1992. — **139**, N 3. — P. 872 — 880.
17. *Yip K.L., Fowler W.B.* // Phys. Rev. B — 1975. — **11**, N 7. — P. 2327 — 2338.
18. *Tsai T.E., Griscom D.L., Friebele E.J. et al.* // J. Appl. Phys. — 1987. — **62**, N 6. — P. 2264 — 2268.
19. *Tsai T.E., Griscom D.L.* // SPIE Proc. — 1991. — **1516**. — P. 14 — 28.
20. *Friebele E.J., Griscom D.L., Sigel Jr. G.H.* // J. Appl. Phys. — 1974. — **45**, N 8. — P. 3424 — 3428.
21. *Fujimaki M., Watanabe T., Katoh T. et al.* // Phys. Rev. B. — 1998. — **57**, N 7. — P. 3920 — 3926.
22. *Purcell T., Weeks R.A.* // Phys. Chem. Glasses. — 1969. — **10**, N 5. — P. 198 — 208.
23. *Griscom D.L.* // J. Ceramic Soc. Jap. — 1991. — **99**, N 10. — P. 923 — 942.
24. *Griscom D.L.* // Phys. Rev. B. — 1979. — **20**, N 5. — P. 1823 — 1834.
25. *Zhang J.Y., Bao X.M., Ye Y.H.* // Thin Solid Films. — 1998. — **323**. — P. 68 — 71.
26. *EerNisse E.P., Norris C.B.* // J. Appl. Phys. — 1974. — **45**, N 12. — P. 5196 — 5205.
27. Ion Implantation and Beam Processing / Ed. by J.S. Williams, J.M. Poate. — New York: Academic Press, 1984.
28. *Ottaviani L., Morvan E., Locatelli M.L. et al.* // Solid-State Electronics. — 1999. — **43**. — P. 2215 — 2223.
29. *Griscom D.L.* // Phys. Rev. B. — 1980. — **22**, N 9. — P. 4192 — 4202.
30. *Zacharias M., Fauchet P.M.* // Appl. Phys. Lett. — 1997. — **71**, N 3. — P. 380 — 382.
31. *Kim H.B., Chae K.H., Whang C.N. et al.* // J. Luminescence. — 1999. — **80**. — P. 281 — 284.

Received 17.01.05.
Translated from Ukrainian by O.I.Voitenko

ЕПР ТА ОПТИЧНІ ДОСЛІДЖЕННЯ ІМПЛАНТОВАНИХ ІОНАМИ ГЕРМАНІЮ ПЛІВОК SiO_2

В.Я. Братусь, М.Я. Валах, Є.Г. Гуле, С.М. Окулов, В.О. Юхимчук

Р е з ю м е

Методами електронного парамагнітного резонансу (ЕПР) та фотолюмінесценції (ФЛ) досліджено вирощені термічним окисленням кремнієвих пластин плівки SiO_2 з рівномірним та близьким до гауссового профілями розподілу імплантованих атомів Ge. Визначено, що основними парамагнітними дефектами є центри E'_γ, пов'язані з вакансією кисню в SiO_2, а також дефекти, зумовлені заміщенням атомами Ge атомів Si в вузлах матриці. Серед них ідентифіковано центри GeE', Ge(2) та германієвий пероксидний радикал (GePR). Динамічним відпалом дефектів у процесі багатоступеневої імплантації пояснюється те, що концентрація дефектів у зразках з рівномірним профілем розподілу атомів Ge на порядок величини менша порівняно зі зразками з гауссовим профілем. Виявлена в процесі відпалу зразків кореляція у зміні інтенсивностей спектрів ЕПР та смуг ФЛ з максимумами 1,94; 2,00 та 2,20 еВ вказує на те, що ці смуги мають дефектну природу. Водночас смуга ФЛ з максимумом 2,32 еВ, яка з'являється після відпалу при 900 °C, пов'язана з утворенням нанокристалітів Ge в SiO_2.